Superconducting transition and phase diagram of single-crystal MgB_2

U. Welp, A. Rydh, G. Karapetrov, W. K. Kwok, and G. W. Crabtree
Materials Science Division, Argonne National Laboratory, Argonne, Illinois 60439

Ch. Marcenat and L. Paulius*
Département de Recherche Fondamentale sur la Matière Condensée, Service de Physique, Magnétisme et Superconductivité, CEA-Grenoble, 38054 Grenoble, France

T. Klein and J. Marcus
Laboratoire d'Etudes des Proprits des Solides, CNRS, BP 166, 38042 Grenoble, France

K. H. P. Kim, C. U. Jung, H.-S. Lee, B. Kang, and S.-I. Lee
NCRICS and Department of Physics, Pohang University of Science and Technology, Pohang 790-784, Republic of Korea
(Received 15 March 2002; published 31 January 2003)

The superconducting phase diagram of MgB_2 was determined from magnetization, magnetotransport, and single-crystal specific-heat measurements. A zero-temperature in-plane coherence length of 9.4 nm is determined. The superconducting anisotropy γ increases from a value around 2 near T_c to above 4.5 at 22 K. For $H\|c$ a pronounced peak effect in the critical current occurs at the upper critical field. Evidence for a surface superconducting state is presented for $H\|c$ that might account for the widespread in reported values of γ.

DOI: 10.1103/PhysRevB.67.012505 PACS number(s): 74.25.Dw, 74.25.Ha, 74.25.Op, 74.25.Qt

MgB_2 has emerged as a fascinating new superconducting material,[1] which in addition to its surprisingly high value of T_c displays a variety of unusual properties. It is characterized by an anisotropic, complex Fermi surface consisting of two disconnected sections: a three-dimensional tubular network of mostly boron π states and two-dimensional cylindrical sheets derived mostly from boron σ states.[2,3] The appearance of multiple superconducting gaps has been predicted,[4] with a large gap residing on the two-dimensional (2D) sheets and a small gap on the 3D network. Specific-heat[5] and spectroscopic measurements[6,7] give evidence for this scenario. In addition, calculations within the anisotropic Eliashberg formalism[8] indicate a strongly anisotropic electron-phonon interaction. However, one of the basic parameters describing an anisotropic superconductor, the anisotropy coefficient $\gamma = H_{c2}^{ab}/H_{c2}^{c}$, is not well established for MgB_2. Here, H_{c2}^{ab} and H_{c2}^{c} are the in-plane and out-of-plane upper critical fields, respectively. Reported values vary widely, ranging from 1.1 to 6 depending on the measurement technique and on sample types.[9–17] Recent torque[13] and thermal conductivity[14] measurements on single crystals as well as magnetization measurements on powders[17] indicate that the anisotropy coefficient is temperature dependent, increasing strongly with decreasing temperature.

Here we present a detailed study of the superconducting phase diagram of MgB_2 combining magnetization $M(T)$, magnetotransport, and single-crystal specific-heat $C_p(T)$ measurements. The transport and magnetization data were taken on the same crystals. The upper critical fields for in- and out-of-plane fields were determined from $M(T)$ and $C_p(T)$ data, yielding a coherence length of $\xi_{ab}(0) = 9.4$ nm. Transport data reveal a pronounced peak effect in the critical current density at H_{c2}^{c}. For fields above H_{c2}^{c}, extending to approximately $1.7H_{c2}^{c}$, we observe strongly non-Ohmic and angular-dependent transport behavior, which we attribute to surface superconductivity. The upward curvature in $H_{c2}^{ab}(T)$ results in a temperature-dependent anisotropy that increases from about 2 near T_c to above 4.5 at 22 K. We note that the occurrence of surface superconductivity could account for the wide variation in reported values for the anisotropy constant.

The MgB_2 crystals were prepared by heat-treating a 1:1 mixture of Mg and B under high-pressure conditions.[18] The crystals are well shaped with straight hexagonal facets and smooth faces [see the picture in the inset of Fig. 1(b)] with a typical size of 50 μm. The magnetization and specific heat were measured in a superconducting quantum-interference device (SQUID) magnetometer and ac specific-heat calorimeter,[19] respectively.

Figure 1(a) shows $M(T)$ measured on warming after field cooling the sample for $H\|c$ and $H\|ab$, respectively. Breaks in the slope of the temperature dependence of the magnetization indicated by the vertical dotted lines are clearly seen and mark the onset of superconductivity. With increasing field there is an essentially parallel shift of the superconducting transition to lower temperatures. This shift is much more pronounced for $H\|c$, indicating a strong superconducting anisotropy of MgB_2 as discussed below. Figure 1(b) shows the heat capacity of a second crystal from the same batch. In zero field a clear step in $C_p(T)$ with a width of about 2 K is observed. With increasing field the step remains well defined and the step height decreases as expected. However, in contrast to results on polycrystalline samples,[5] the width remains essentially constant. Defining T_c using an entropy conserving construction[19] a phase boundary is obtained that agrees with that determined from $M(T)$ as discussed below. Thus, the data shown in Fig. 1 represent the thermodynamic bulk transition of MgB_2 into the superconducting state.

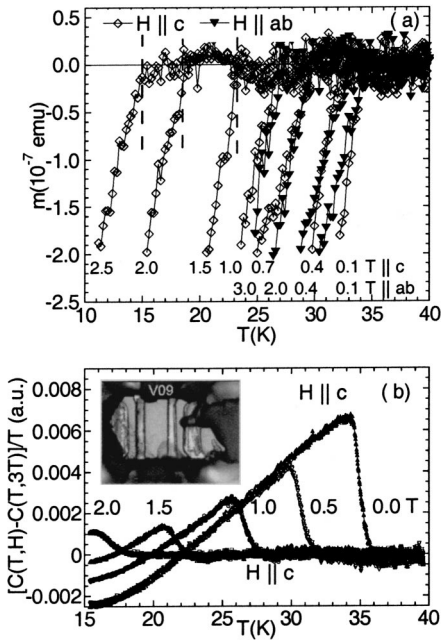

FIG. 1. (a) Temperature dependence of the magnetic moment in the indicated fields parallel c (open symbols) and parallel ab (solid symbols). The inset in (b) shows a photo of the crystal. The smooth faces and the Au contacts are seen. The irregular shaped features on the surface are glue residues. (b) Temperature dependence of the heat capacity in several fields. The 3 T data were used to subtract the background signal.

Figure 2 shows the resistive transitions in various fields along the c axis. The sample is characterized by a resistivity of $\rho = 1.6\ \mu\Omega$ cm at 40 K. With increasing field the resistive transition moves to lower temperature and broadens significantly. A similar broadening has been observed in previous studies on single crystals.[10,11] However, here we show that the broadening is strongly current dependent. Non-Ohmic behavior appears at the onset of the transition, labeled $T_{\rm on}$. With increasing current a steep resistive drop emerges at a

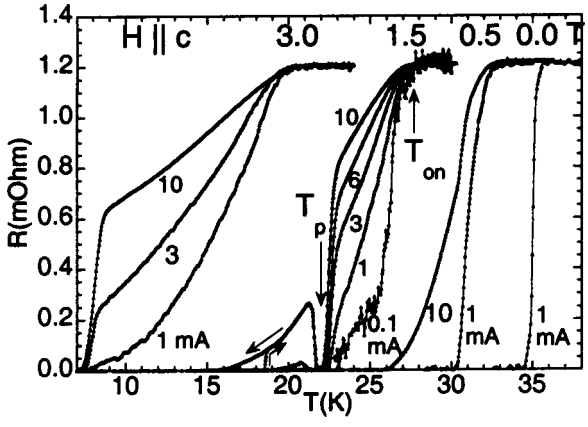

FIG. 2. Resistive transition measured on cooling in various fields and current densities, 1 mA equals 360 A/cm^2. The onset of non-Ohmic behavior at T_{on} and the peak effect at T_p are indicated. At 1.5 T and 10 mA the hysteresis arising between cooling and warming is indicated by arrows.

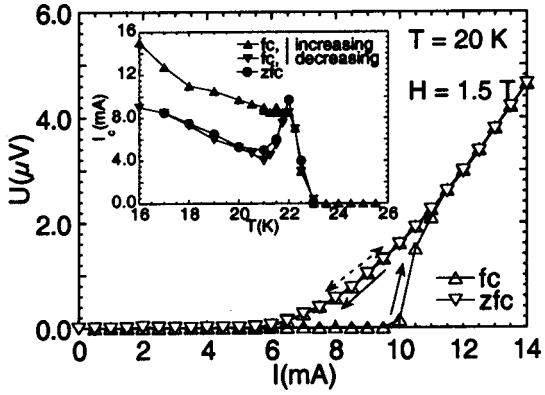

FIG. 3. I-V characteristics at 20 K and 1.5 T$\|c$ measured for increasing and decreasing current after field cooling (solid arrows) and after zero-field cooling (dashed arrows). The inset shows the temperature dependence of the critical current in 1.5 T$\|c$.

lower, almost current-independent temperature. At even higher currents a nonmonotonic, hysteretic resistivity behavior arises that is reminiscent of the peak effect. Peak effects, that is, sharp maxima in the temperature and/or field dependence of the critical current, have been observed just below $H_{c2}(T)$ in a variety of low pinning superconductors, including $NbSe_2$ (Refs. 20 and 21) and borocarbides (Ref. 22). For $H\|ab$ the resistive transitions do not broaden, in agreement with previous reports.[10,11]

Figure 3 summarizes the transport behavior in the peak-effect region at 1.5 T$\|c$. The current-voltage (I-V) characteristics after field-cooling to 20 K display pronounced hysteretic behavior. On first increasing the current, a sharp onset of dissipation occurs near a critical current of 10 mA, whereas for decreasing current zero dissipation is approached near 5.5 mA. All subsequent current ramps and also the I-V characteristics taken after zero-field cooling follow this curve. These results are a manifestation of a current-induced transition from a metastable high-I_c vortex phase into a stable low-I_c phase. As the sample is field-cooled through $T_{c2}(H)$ a high-pinning vortex phase nucleates and stays in thermodynamic equilibrium until the peak-effect temperature is reached (see inset of Fig. 3). At lower temperatures this phase may survive as a supercooled metastable state. The application of a strong enough current dislodges vortices from their pinned metastable configuration and triggers a transition into the stable low-pinning state, which does not change on subsequent current ramps. In zero-field-cooled measurements the initial vortex configuration is the result of flux-gradient driven motion of vortices across the sample, and a low-pinning state analogous to the current-induced state is created. Thus, the zero-field-cooled I-V characteristic coincides with the stable field-cooled I-V characteristic. Similar results have been reported for $NbSe_2$ (Ref. 21) when fast current ramps are applied, whereas the data in Fig. 3 represent steady states with the applied current set point-by-point. This difference is caused by the stronger pinning ($j_c \approx 3000$ A/cm^2) in our MgB_2 crystal than typically seen in $NbSe_2$ ($j_c \approx 50$ A/cm^2). Recently, peak effects in also the magnetic response of MgB_2 have been reported.[23]

The magnetic, calorimetric, and transport data are sum-

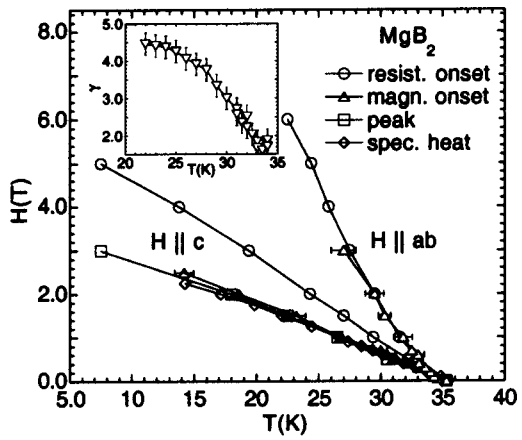

FIG. 4. Superconducting phase diagram of MgB_2 as determined from the magnetization, specific-heat, and transport measurements.

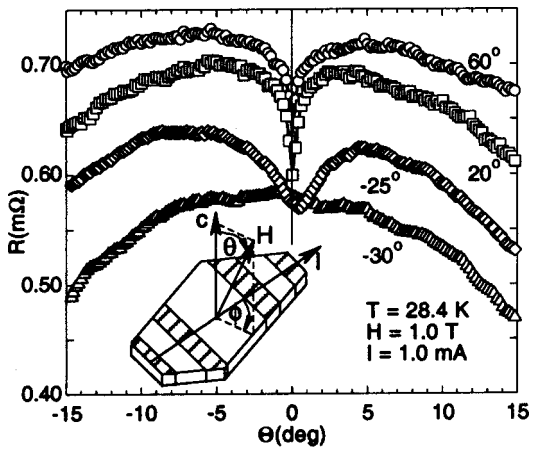

FIG. 5. Angular dependence of the resistance. The inset shows the sample geometry. The corners of the crystal make angles of 120°, and the electrical contacts are marked by cross-hatches. Θ is the polar angle with respect to the c axis and ϕ is the azimuthal angle with respect to the net current direction. Surface superconductivity on the vertical side faces is probed in these data.

marized in the phase diagram shown in Fig. 4. For $H\|c$ the onsets of superconductivity as determined from $M(T)$ and $C_p(T)$ coincide with each other and with the location of the peak effect within the experimental uncertainty. We identify this line with the upper critical field for the c axis, $H_{c2}^c(T)$. A zero-temperature value of $H_{c2}^c(0)\approx 3.5$ T can be estimated, which, using the relation $H_{c2}^c(0)=\Phi_0/2\pi\xi_{ab}^2(0)$, yields the zero-temperature coherence length $\xi_{ab}(0)\approx 9.4$ nm.

While the upper critical field for $H\|c$ follows a conventional temperature dependence, a pronounced upward curvature of $H_{c2}(T)$ was observed for the *ab* directions. As a result the superconducting anisotropy is temperature dependent as shown in the inset of Fig. 4. Similar results have recently been obtained from torque,[13] magnetization,[17] and thermal conductivity[14] measurements. At high temperatures γ has a value between 1.5 and 2 and reaches values above 4.5 near 22 K. An upward curvature of the $H_{c2}(T)$ line and temperature-dependent anisotropy have been observed in clean, layered superconductors such as $NbSe_2$ (Ref. 24) and borocarbides (Refs. 25 and 26). These features, which cannot be accounted for with standard effective mass anisotropy, can arise from[28] nonlocal corrections, gap anisotropy, or multiband effects. A two-band model[26,27] may explain the properties of MgB_2 since its electron system naturally falls into two groups. At low temperatures and high fields the upper critical field is dominated by the highly anisotropic 2D bands (the 3D gap being largely suppressed in high fields[5,6]), resulting in the large measured values of the anisotropy. At high temperatures, near T_c, the superconducting transition involves the entire Fermi surface, including the 3D band, resulting in a reduced anisotropy.

The onset of non-Ohmic transport with decreasing temperature defines a line in the phase diagram lying by a factor 1.66 above the H_{c2}^c line. This suggests that the resistive onset is a manifestation of surface superconductivity[29] at H_{c3}, which for a flat surface in parallel magnetic field occurs at $1.7H_{c2}$. For $H\|c$ the surface superconducting currents are flowing on the vertical side faces of the platelike crystals. Although resistive transitions as shown in Fig. 2 could in principle result from filamentary conduction along impurity phases, the observation of a single sharp, current-independent superconducting transition in zero field indicates an intrinsic mechanism. Nearly identical resistivity results were obtained on a second, smaller crystal. We also note that the limits of the resistive broadening reported earlier[10] encompass the same coefficient, 1.7. Furthermore, non-Ohmic transport data above the bulk upper critical field have been reported for NbTa and PbIn samples.[30] These results, closely resembling those in Fig. 2, have been interpreted as a signature of surface superconductivity.

Further evidence for a surface superconducting state comes from the angular dependence of the resistivity of a third crystal measured in the regime of non-Ohmic transport above the bulk upper critical field (Fig. 5). Pronounced cusp-like dips in the resistance with a width of less than 3° are observed when the field is aligned with the c axis. With increasing angle Θ the resistance increases rapidly and at high angles decreases again due to the superconducting anisotropy of MgB_2. This kind of angular dependence could be caused by extended crystal defects containing the c axis such as small-angle grain boundaries. However, x-ray diffraction reveals a very high quality of the crystals without any indication for this type of defects.[18] Furthermore, the dip is strongly dependent on the azimuthal angle ϕ. It is most pronounced when the field is tilted in a plane perpendicular to the side face ($\phi=60°$) and is absent for tilt in the plane of the side face ($\phi=-30°$). This behavior is expected for a surface superconducting state. The highest nucleation field for surface superconductivity occurs for fields applied parallel to the surface. The surface superconducting state is rapidly suppressed with increasing angle α between field and surface.[31] For the geometry in Fig. 5, α is given through $\sin(\alpha)=\sin(\Theta)\sin(\phi+30°)$. Thus, for $\phi=-30°$, we get $\alpha=0$, and the surface superconducting state is fully developed, implying a low resistance. Angular dependence arises only from the intrinsic anisotropy of MgB_2. For other azimuthal angles, α grows with Θ, causing the rapid suppression of surface superconductivity and a steep increase in the resis-

tance. In fact, if these data are replotted as a function of α, their initial slopes coincide, as is expected.

Reported γ values determined from resistivity measurements (usually the resistive onset[9–12,15] is identified with H_{c2}) are generally low, in the range of 2–3. In contrast, magnetic measurements[13,16,17] as well as thermal conductivity measurements[14] yield γ values around 6 at low temperatures. Since surface superconductivity does not contribute to the magnetization[29] nor the thermal conductivity of bulk samples but does induce nonlinear response in the resistivity, a discrepancy between both determinations is expected.

In conclusion, a comprehensive superconducting phase diagram of MgB_2 has been determined using magnetization, magnetotransport, and single-crystal specific-heat measurements. The in-plane coherence length is 9.4 nm corresponding to $H_{c2}^{c}(0) \approx 3.5$ T. The superconducting anisotropy increases with decreasing temperature from a value around 2 near T_c to above 4.5 at 22 K. For $H \| c$ a pronounced peak effect in the critical current occurs at the upper critical field. Evidence for a surface superconducting state is presented for $H \| c$, which might account for the widespread of reported values for the anisotropy coefficient.

This work was supported by the U.S. Department of Energy, BES, Materials Science under Contract No. W-31-109-ENG-38, by the National Science Foundation under Grant No. 0072880, the Fulbright Program (A.R.), and by the Ministry of Science and Technology of Korea through the Creative Research Initiative Program.

*Permanent address: Department of Physics, Western Michigan University, Kalamazoo, MI 49008.

[1] J. Nagamatsu *et al.*, Nature (London) **410**, 63 (2001).
[2] J. M. An and W. E. Pickett, Phys. Rev. Lett. **86**, 4366 (2001); J. Kortus *et al.*, *ibid.* **86**, 4656 (2001).
[3] E. A. Yelland *et al.*, Phys. Rev. Lett. **88**, 217002 (2002).
[4] A. Y. Liu *et al.*, Phys. Rev. Lett. **87**, 087005 (2001).
[5] F. Bouquet *et al.*, Phys. Rev. Lett. **87**, 047001 (2001); Y. Wang *et al.*, Physica C **355C**, 179 (2001).
[6] P. Szabo *et al.*, Phys. Rev. Lett. **87**, 137005 (2001).
[7] F. Giubileo *et al.*, Phys. Rev. Lett. **87**, 177008 (2001); X. K. Chen *et al.*, *ibid.* **87**, 157002 (2001); H. Schmidt *et al.*, *ibid.* **88**, 127002 (2002); M. Iavarone *et al.*, Phys. Rev. Lett. **89**, 187002 (2002).
[8] H. J. Choi *et al.*, Nature (London) **418**, 758 (2002).
[9] K. H. P. Kim *et al.*, Phys. Rev. B **65**, 100510 (2002).
[10] S. Lee *et al.*, J. Phys. Soc. Jpn. **70**, 2255 (2001); Yu. Eltsev *et al.*, Phys. Rev. B **65**, 140501 (2002).
[11] A. K. Pradhan *et al.*, Phys. Rev. B **64**, 212509 (2001).
[12] M. Xu *et al.*, Appl. Phys. Lett. **79**, 2779 (2001).
[13] M. Angst *et al.*, Phys. Rev. Lett. **88**, 167004 (2002).
[14] A. V. Sologubenko *et al.*, Phys. Rev. B **65**, 180505 (2002).
[15] S. Patnaik *et al.*, Semicond. Sci. Technol. **14**, 315 (2001); M. H. Jung *et al.*, Chem. Phys. Lett. **343**, 447 (2001).
[16] F. Simon *et al.*, Phys. Rev. Lett. **87**, 047002 (2001); S. L. Bud'ko *et al.*, Phys. Rev. B **64**, 180506 (2001).
[17] S. L. Bud'ko *et al.*, cond-mat/0201085 (unpublished).
[18] C. U. Jung *et al.*, cond-mat/0203123 (unpublished).
[19] F. Bouquet *et al.*, Nature (London) **411**, 448 (2001).
[20] M. Higgins and S. Bhattacharya, Physica C **257**, 232 (1996); X. S. Ling *et al.*, Phys. Rev. B **57**, 3249 (1998); Y. Paltiel *et al.*, Phys. Rev. Lett. **85**, 3712 (2000).
[21] Z. L. Xiao *et al.*, Phys. Rev. Lett. **85**, 3265 (2000).
[22] K. J. Song *et al.*, Phys. Rev. B **59**, 6620 (1999); S. S. James *et al.*, Physica C **332**, 173 (2000).
[23] M. Pissas *et al.*, Phys. Rev. Lett. **89**, 097002 (2002); L. Lyard *et al.*, Phys. Rev. B **66**, 180502 (2002).
[24] Y. Muto *et al.*, Phys. Lett. A **45**, 99 (1973); J. A. Wollam *et al.*, Phys. Rev. Lett. **32**, 712 (1974).
[25] V. Metlushko *et al.*, Phys. Rev. Lett. **79**, 1738 (1997).
[26] S. V. Shulga *et al.*, Phys. Rev. Lett. **80**, 1730 (1998).
[27] P. Miranovic *et al.*, cond-mat/0207146 (unpublished).
[28] *Anisotropy Effects in Superconductors*, edited by H. W. Weber (Plenum, New York, 1977).
[29] D. Saint-James and P. G. de Gennes, Phys. Lett. **7**, 306 (1963); A. Abrikosov, Zh. Eksp. Teor. Fiz. **47**, 720 (1964) [Sov. Phys. JETP **20**, 480 (1965)].
[30] C. Hempstead and Y. Kim, Phys. Rev. Lett. **12**, 145 (1964).
[31] R. S. Thompson, Zh. Eksp. Teor. Fiz. **69**, 2249 (1975) [Sov. Phys. JETP **42**, 1144 (1976)].